Medical Engineering & Physics 32 (2010) 136–144

Contents lists available at ScienceDirect

Medical Engineering & Physics

journal homepage: www.elsevier.com/locate/medengphy

Analysis of unpredictable intra-QRS potentials in signal-averaged electrocardiograms using an autoregressive moving average prediction model

Chun-Cheng Lin*

Department of Electrical Engineering, National Chin-Yi University of Technology, No. 35, Lane 215, Sec. 1, Jhongshan Rd., Taiping City, Taichung County 411, Taiwan

ARTICLE INFO

Article history:
Received 16 July 2009
Received in revised form
22 September 2009
Accepted 2 November 2009

Keywords:
Signal-averaged electrocardiogram
Unpredictable intra-QRS potentials
Abnormal intra-QRS potentials
Ventricular tachycardia
Autoregressive moving average prediction model

ABSTRACT

Instead of extracting the abnormal intra-QRS potentials (AIQP) waveform, this study proposes the analysis of the unpredictable intra-QRS potentials (UIQP) based on an autoregressive moving average (ARMA) prediction model to detect the signals with sudden slope change within the QRS complex for the diagnosis of high-risk patients with ventricular tachycardia (VT). The UIQP is detected as the slope changes at slope discontinuities by the prediction error of the ARMA prediction model. Because of the linearity of the ARMA prediction model, the UIQP is also proportional to the amplitude of the QRS complex if the input QRS waves have the same shapes. Hence this study further defines the UIQP-to-QRS ratio to normalize the UIQP by the root-mean-square (RMS) value of the QRS complex. The study subjects were composed of 42 normal Taiwanese and 30 patients with sustained VT. The clinical results show that the UIQP-to-QRS ratios of the VT patients in leads X, Y and Z were significantly higher than those of the normal subjects. The logical combination of any 4 of the UIQP-to-QRS ratios and conventional time-domain parameters can increase the diagnosis performance of VT patients to 92.9% specificity, 93.3% sensitivity and 93.1% total prediction accuracy.

1. Introduction

Ventricular late potentials (VLP) in signal-averaged electrocardiograms (SAECG) which outlast the normal QRS interval have been an important and non-invasive marker for the risk stratification of ventricular arrhythmias to prevent sudden cardiac death [1–4]. According to the recommendations of an ACC Expert Consensus Document [4] for the use of SAECG, the established clinical values are for the stratification of the risk of development of sustained ventricular arrhythmias in patients who are recovering from myocardial infarction, and for the identification of patients with ischemic heart disease and unexplained syncope. Several recent studies further applied time-domain VLP analysis to evaluate the risk of ventricular arrhythmias for symptomatic and asymptomatic patients with Brugada syndrome [5], Chagas disease patients [6], thalassemia patients [7] and patients with arrhythmogenic right ventricular cardiomyopathy [8].

However, the weakness of VLP analysis is the low positive predictive accuracy [4] and the incomplete characterization of reentrant activity [9]. The VLP may be completely contained within the normal QRS complex and not prolong the normal QRS interval [10,11]. In recent years, several studies [12–15] have also been focused on the analysis of the abnormal intra-QRS potentials (AIQP) which are considered as low-amplitude notches and slurs with sudden changes in slope, to enhance the diagnostic performance of SAECG. The AIQP analysis has also been applied to noninvasively identify the mechanisms of premature ventricular beats (PVBs) [16] and to detect acute transmural myocardial ischemia [17].

The current autoregressive moving average (ARMA) modeling technique in the discrete cosine transform (DCT) domain [12] for extracting the AIQP can use a low model order to estimate the normal QRS complex and then separate out the AIQP. However, the true model order is unknown. Although our previous study [14] proposed a cross correlation method to automatically determine the model order, it cannot verify if the determined order is correct. The estimated AIQP may also contain a high estimation error due to the overlap between the normal QRS complex and the AIQP in the DCT domain [15]. Hence it is not an easy job to accurately extract the AIQP waveform, particularly with an extremely poor signal–noise-ratio (low-amplitude AIQP compared with a large QRS wave).

Instead of extracting the AIQP waveform, this study proposes the analysis of unpredictable intra-QRS potentials (UIQP) based on an autoregressive moving average prediction model to detect the signals with sudden slope change, which originate from the sharp QRS wave and the AIQP, for the diagnosis of high-risk patients with ventricular tachycardia (VT). The VT patients are expected to have higher UIQP because the presence of AIQP would bring more components with sudden changes in slope within the QRS complex. The

* Tel.: +886 4 23924505x7238; fax: +886 4 23924419.
E-mail address: cclin@ncut.edu.tw.

1350-4533/$ – see front matter © 2009 IPEM. Published by Elsevier Ltd. All rights reserved.
doi:10.1016/j.medengphy.2009.11.001

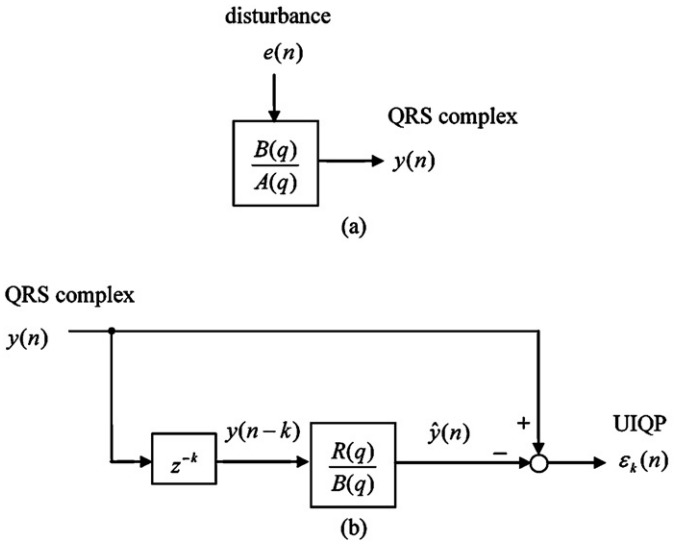

Fig. 1. Block diagrams of (a) a single-output ARMA model of the QRS complex and (b) an ARMA prediction model for the extraction of UIQP.

aim of this study is to determine whether the UIQP detected as the slope changes at slope discontinuities by the prediction error of an ARMA prediction model can be applied to diagnose the VT patients and to improve the diagnostic performance of SAECG.

2. Methods

2.1. Data acquisition

This work followed the principles that (1) informed consent was obtained from each patient and (2) the Ethics Committee of Taipei Jen-Chi General Hospital had approved the study. The study subjects recruited were 42 normal Taiwanese (20 men and 22 women, aged 58 ± 14 years) and 30 patients with sustained VT (15 men and 15 women, aged 63 ± 16 years). The VT patients were suffering from chronic ischemic heart disease after surviving clinically documented myocardial infarction (MI). These study subjects were identical with the previous study [15].

The high-resolution ECGs were recorded at rest in a supine position using a commercially available Simens-Elema Megacart® machine and a bipolar, orthogonal X-, Y- and Z-lead system, and were digitized with a 2 kHz sampling rate and 12-bit resolution. The time unit was 0.5 ms per sample. The signal averaging technique was used to lower the effects of the random noise. According to the standards of SAECG analysis recommended by the 1991 ESC, AHA and ACC Task Force [3], the final noise level measured with a 40–250 Hz bidirectional Butterworth filter was reduced to less than 0.7 μV in this study. The onset and offset of the signal-averaged QRS wave were obtained from vector magnitude analysis. Three standardized time-domain VLP parameters, namely filtered total QRS duration (fQRSD), RMS voltage of the last QRS 40 ms (RMS40), and duration of the low-amplitude signals below 40 mV (LAS40), were analyzed [3,4].

2.2. Development of the ARMA prediction modeling technique

The proposed ARMA prediction model is derived from the optimization of a single-output ARMA model. The single-output ARMA model shown in Fig. 1(a) can be expressed as [18]

$$A(q)y(n) = B(q)e(n) \tag{1}$$

where $y(n)$ is the output and also the QRS complex, and $e(n)$ is the unmeasured disturbance. The system model, $A(q)$, and the noise model, $B(q)$ are polynomials in q^{-1} given by

$$A(q) = 1 + a_1 q^{-1} + \ldots + a_{na} q^{-na} \tag{2}$$

$$B(q) = 1 + b_1 q^{-1} + \ldots + b_{nb} q^{-nb} \tag{3}$$

where the backward shift operator, q^{-1}, shifts time backward by one sample, i.e., $q^{-1}w(n) = w(n-1)$. One way to evaluate how well the model fits the QRS complex is to analyze the prediction ability of the model. If we express the output $y(n)$ as

$$y(n) = H(q)e(n) = \sum_{l=0}^{\infty} h(l)e(n-l) = e(n) + \sum_{l=1}^{\infty} h(l)e(n-l) \tag{4}$$

where

$$H(q) = \frac{B(q)}{A(q)} = \sum_{l=0}^{\infty} h(l)q^{-l} \text{ and } h(0) = 1, \tag{5}$$

a one-step-ahead predictor using the observations of $y(s)$ and $e(s)$ for $s \le n-1$ to predict $y(n)$ can be defined by

$$\hat{y}(n) = \sum_{l=1}^{\infty} h(l)e(n-l) = [H(q) - 1]e(n)$$

$$= [1 - H^{-1}(q)]y(n) = \left[1 - \frac{A(q)}{B(q)}\right] y(n) \tag{6}$$

Given a specific set of model order (na, nb), the coefficients of the polynomials $A(q)$ and $B(q)$ can be estimated using iterative optimization methods for minimizing the prediction error ($\varepsilon(n) = y(n) - \hat{y}(n)$) in the least-square sense, with the nonlinear criterion function

$$V(\theta) = \frac{1}{N}\sum_{n=1}^{N}\frac{1}{2}\varepsilon^2(n) = \frac{1}{N}\sum_{n=1}^{N}\frac{1}{2}\left[\frac{A(q^{-1})}{B(q^{-1})}y(n)\right]^2 \tag{7}$$

This study used a Gauss–Newton algorithm, based on the gradient and Hessian of the criterion function to search for the optimal parameters iteratively [18].

The ARMA prediction model with various prediction depths can be further derived using the optimized polynomials of $A(q)$ and $B(q)$. If we express the QRS complex as

$$y(n) = \sum_{l=0}^{k-1} h(l)e(n-l) + \sum_{l=k}^{\infty} h(l)e(n-l) \tag{8}$$

and use the notations

$$\tilde{H}_k(q) = \sum_{l=0}^{k-1} h(l)q^{-l} \text{ and } \tilde{H}_k(q) = \sum_{l=k}^{\infty} h(l)q^{-l+k}, \tag{9}$$

a k-step-ahead predictor can be defined by

$$\hat{y}(n) = \sum_{l=k}^{\infty} h(l)e(n-l) = \tilde{H}_k(q)e(n-k) = \tilde{H}_k(q)H^{-1}(q)y(n-k). \tag{10}$$

Because $H(q) = \tilde{H}_k(q) + q^{-k}\tilde{H}_k(q)$ and the polynomial division of $B(q)/A(q)$ can be expressed as

$$\frac{B(q)}{A(q)} = \tilde{H}_k(q) + \frac{q^{-k}R(q)}{A(q)} \tag{11}$$

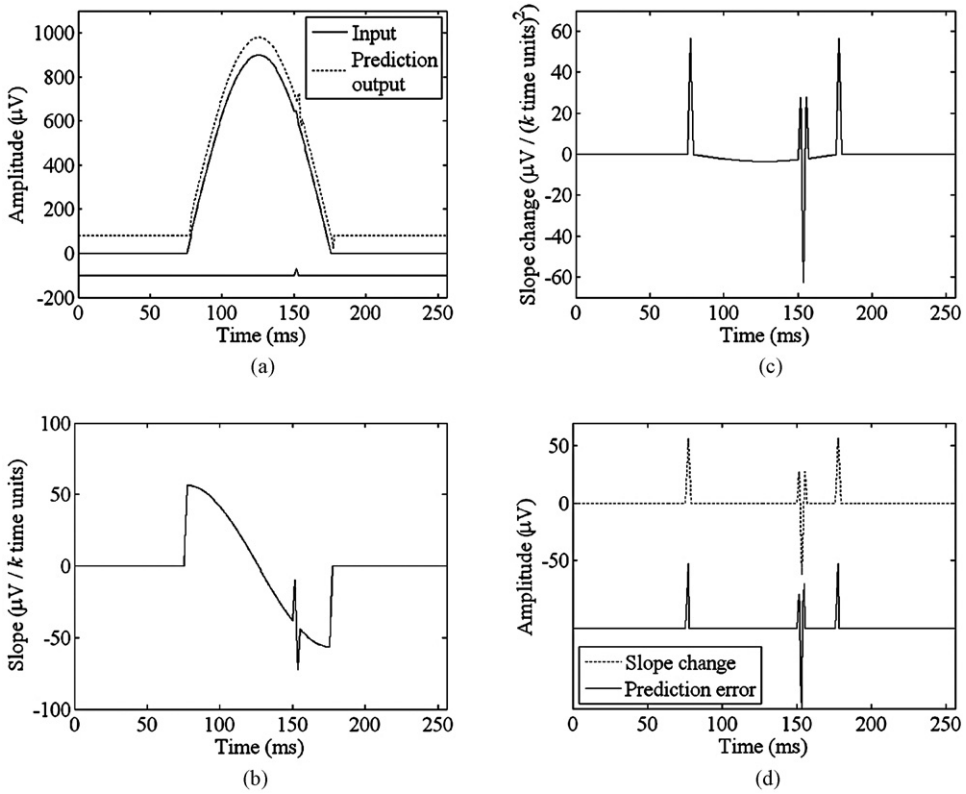

Fig. 2. Prediction results for the input of a positive sinusoidal wave adding a low-amplitude triangle wave located at time 150 ms using an ARMA prediction model of order $na = 10$, $nb = 1$ and prediction depth $k = 4$: (a) the input signal (solid line) and the prediction output (dotted line); (b) the slope function and (c) the slope change function of the input signal; (d) the slope changes at slope discontinuities (solid line) and the prediction error (dotted line).

where $\tilde{H}_k(q)$ is the quotient polynomial of order $k-1$, and $q^{-k}R(q)$ is the remainder polynomial given by

$$R(q) = \sum_{l=k}^{k+na+1} r(l)q^{-l+k}, \tag{12}$$

we can obtain

$$\tilde{H}_k(q) = \frac{R(q)}{A(q)}. \tag{13}$$

By substituting Eq. (13) into Eq. (10), the k-step-ahead predictor can be simplified as

$$\hat{y}(n) = \frac{R(q)}{B(q)}y(n-k) \tag{14}$$

Hence if the optimal coefficients of the polynomials $A(q)$ and $B(q)$ are determined, the use of Eqs. (11) and (14) can provide a convenient way to calculate the prediction output for various prediction depths. Fig. 1(b) shows the block diagram of an ARMA prediction model with the prediction depth k. The prediction error is used for the analysis of UIQP and can be obtained by

$$\varepsilon_k(n) = y(n) - \hat{y}(n) \tag{15}$$

To demonstrate that the minimized prediction error can be used to detect the slope changes at the slope discontinuities of the input signal, this study particularly defined a slope function as the amplitude changes per k time units,

$$s(n) = y(n) - y(n-k), \tag{16}$$

and a slope change function as the slope changes per k time units,

$$a(n) = s(n) - s(n-k). \tag{17}$$

2.3. Definition of UIQP parameters

This study introduced the prediction error of the ARMA prediction model with various prediction depths to analyze the UIQP for the diagnosis of VT patients. A root-mean-square value (RMS) of the prediction error within the entire QRS duration, UIOP_*l*, and a UIQP-to-QRS ratio, UQR_*l*, were defined to quantify the UIQP as follows,

$$\text{UIQP\_}l = \sqrt{\frac{1}{\text{fQRSD}}\sum_{n=n_1}^{n_2}\varepsilon_k^2(n)} \tag{18}$$

and

$$\text{UQR\_}l = \frac{\text{UIQP\_}l}{\sqrt{(1/\text{fQRSD})\sum_{n=n_1}^{n_2}y^2(n)}} \tag{19}$$

where l denotes lead X, Y or Z, n_1 and n_2 are the onset and offset of the QRS complex respectively, $\varepsilon_k(n)$ is the prediction error using the prediction depth k, and $y(n)$ is the input QRS complex.

2.4. Statistical methods

This study applied Fisher's linear discriminant analysis to combine the time-domain VLP and UIQP parameters and to classify the normal and VT groups [19]. Pearson's product moment correlation coefficient ρ was employed to measure the level of linear correlation. Three clinical performance indices including specificity, sensitivity and total prediction accuracy (TPA) [20] were calculated to evaluate the accuracy of the diagnosis of the VT patients.

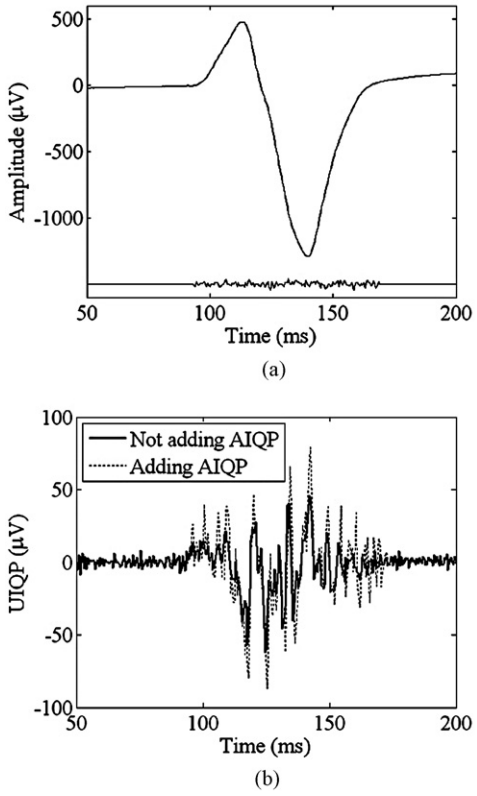

Fig. 3. Comparisons of the UIQPs for a normal QRS complex adding and not adding the simulated AIQP: (a) a Z lead QRS complex of a normal subject simulating the normal QRS complex and a normally distributed white noise with zero mean simulating the AIQP; (b) the UIQPs estimated by an ARMA prediction model of order $na = 10$, $nb = 1$ and the prediction depths $k = 4$ for the QRS complex adding (dashed line) and not adding (solid line) AIQP.

3. Results

3.1. Simulation analyses

To demonstrate the signals that can and cannot be predicted by an ARMA prediction model, this study used a positive sinusoidal wave of 900 μV peak value and 100 ms duration to simulate a smoothed R wave, and a low-amplitude, transient positive triangular wave of 30 μV peak value and 2.5 ms duration to simulate the AIQP. The simulated AIQP was located at time 150 ms. Fig. 2(a) shows the synthesized input signal (solid line) and the prediction output (dashed line) of an ARMA prediction model of order $na = 10$, $nb = 1$ and prediction depth $k = 4$. Fig. 2(b) and (c) plots the slope and slope change functions of the input signal defined in Eqs. (15) and (16), respectively. It can be found that the main prediction error points were located at slope discontinuities including the starting and end points of the positive sinusoidal wave, and the simulated AIQP. Fig. 2(d) compares the prediction error (solid line) with the slope change at slope discontinuities (dashed line). If the smoothed part of the input signal can be accurately predicted by the ARMA prediction model, the prediction error can be applied to detect the slope changes at the slope discontinuities. It can also be observed that there are k data points exhibiting prediction errors at each slope discontinuity, and the prediction error at the kth data point is close to $(k/2) \times (m_2 - m_1)$ if the slope is suddenly changed from m_1 to m_2. Hence a larger prediction depth produces larger prediction errors and more error points at each slope discontinuity.

This study further used a Z lead QRS complex with an RMS value of 600 μV from the normal subjects to simulate the normal QRS complex. Because the true waveform and randomness of AIQP are unknown, this study introduces a normally distributed white noise with zero mean and RMS value of 3 μV to simulate the AIQP. Fig. 3(a) shows the simulated QRS complex and AIQP. Fig. 3(b) compares the

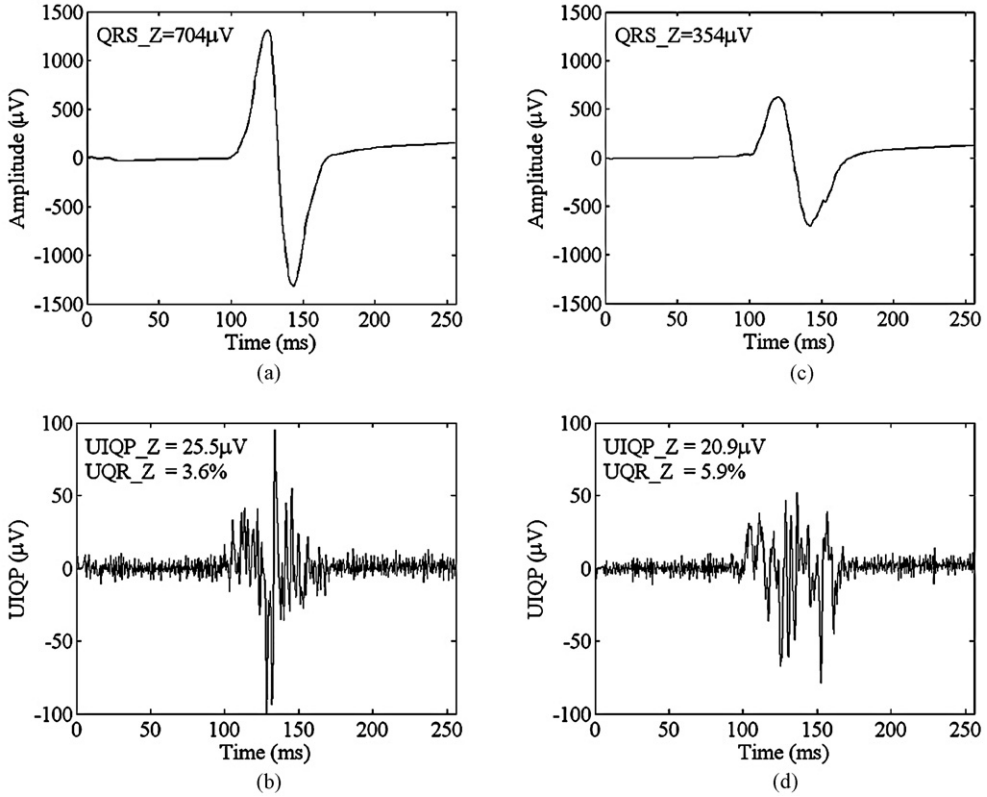

Fig. 4. Comparisons of the QRS waves and UIQPs for a normal subject and a VT patient in lead Z: (a) the QRS wave and (b) the UIQP of a normal subject, and (c) the QRS wave and (d) the UIQP of a VT patient. The UIQPs were estimated by an ARMA prediction model of order $na = 10$, $nb = 1$ and the prediction depths $k = 4$.

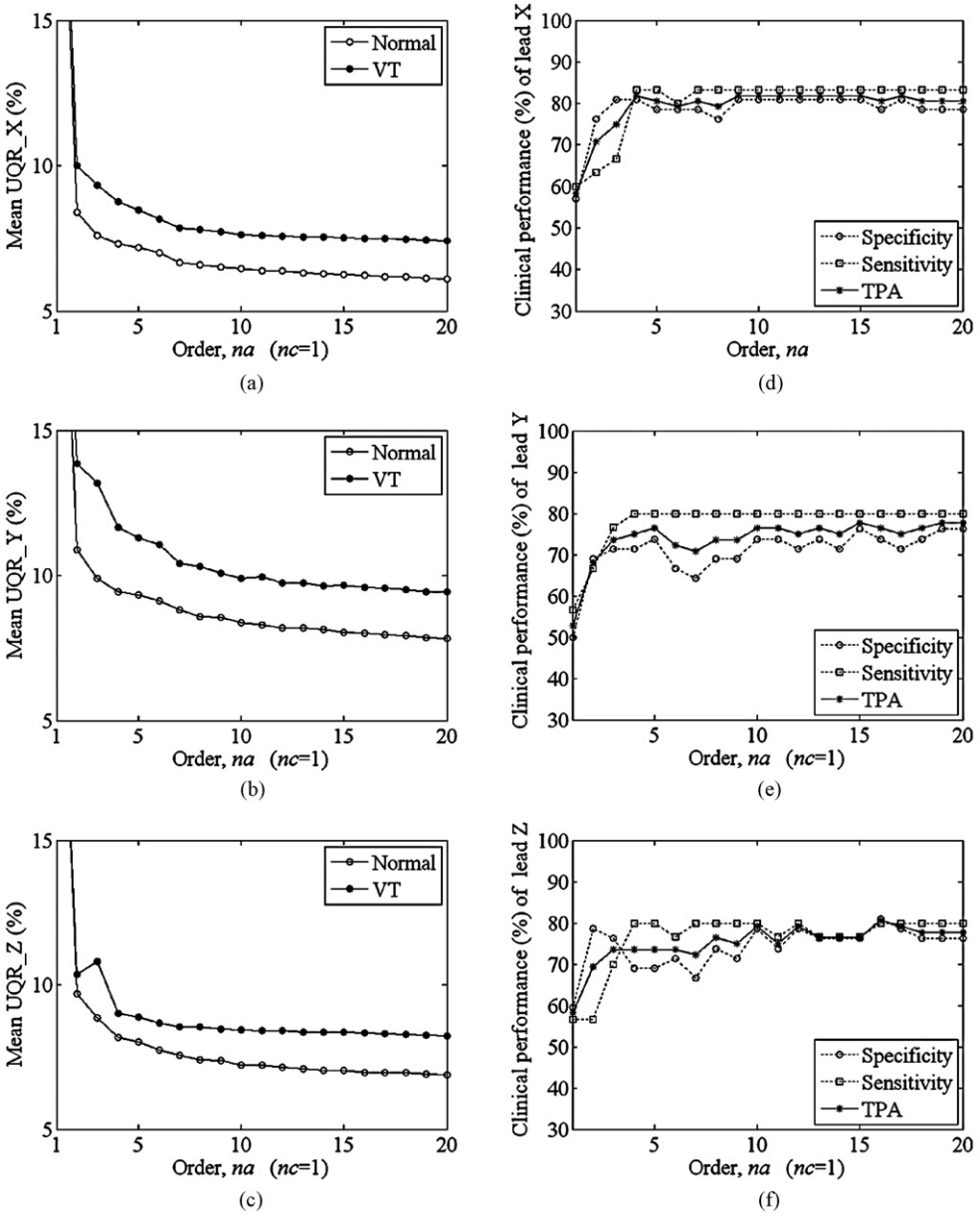

Fig. 5. Analysis of the model order *na* vs. (a)–(c) mean UIQP-to-QRS ratios and (d)–(f) clinical performance in leads X, Y and Z. The prediction depth *k* of 6 and the order *nb* of 1 are fixed.

UIQPs for the QRS complex adding (dashed line) and not adding (solid line) AIQP, using an ARMA prediction model of order $na = 10$, $nb = 1$ and the prediction depth $k = 4$. The RMS values of the input QRS complex were adjusted to be equal to 600 μV, and the QRS complex with AIQP revealed a higher RMS value of UIQP in comparison with one without AIQP, 27.2 μV vs. 18.8 μV, respectively. However if the input QRS complexes have the same shapes, the UIQPs are proportional to the amplitude of the input QRS complexes because of the linearity of the ARMA prediction model. For example, if the RMS value of the normal QRS complex in Fig. 3(a) is amplified 2 times to 1200 μV, the RMS value of UIQP is increased to 37.6 μV. If we only compare the RMS values of UIQP, the normal QRS complex with RMS value of 1200 μV would be misclassified as being in the VT group. This study further defined a UIQP-to-QRS ratio in Eq. (18) to normalize the UIQP parameters. The UIQP-to-QRS ratio after adding the simulated AIQP was 4.5%, which is higher than the 3.1% of the normal QRS complex.

Fig. 4 compares the QRS waves and UIQPs for a normal subject and a VT patient in lead Z. The UIQP was estimated by an ARMA prediction model of order $na = 10$, $nb = 1$ and prediction depths $k = 4$. Fig. 4(a) and (c) plots the Z lead QRS waves of a normal subject and a VT patient, and the RMS values of the QRS wave were 704 μV and 354 μV, respectively. Although the VT patient was expected to have a higher UIQP in comparison with the normal subject due to the existence of the AIQP, the RMS value of the UIQP for this VT patient (Fig. 4(b)) was 20.9 μV which was not higher than that of the normal subject, 25.5 μV (Fig. 4(d)). Hence this VT patient cannot obtain a correct diagnosis from the UIQP parameter. However if the UIQP parameter was normalized by the RMS value of the QRS wave, this VT patient showed a higher UIQP-to-QRS ratio of 5.9% in comparison with 3.6% of the normal subject.

3.2. Determination of model order and prediction depth

The model orders *na* and *nb*, and prediction depth *k* are the major parameters of the ARMA prediction model. The model order must be sufficient to accurately predict the smoothed components of the QRS complex. Figs. 5 and 6 use various orders *na* and *nb* to compare

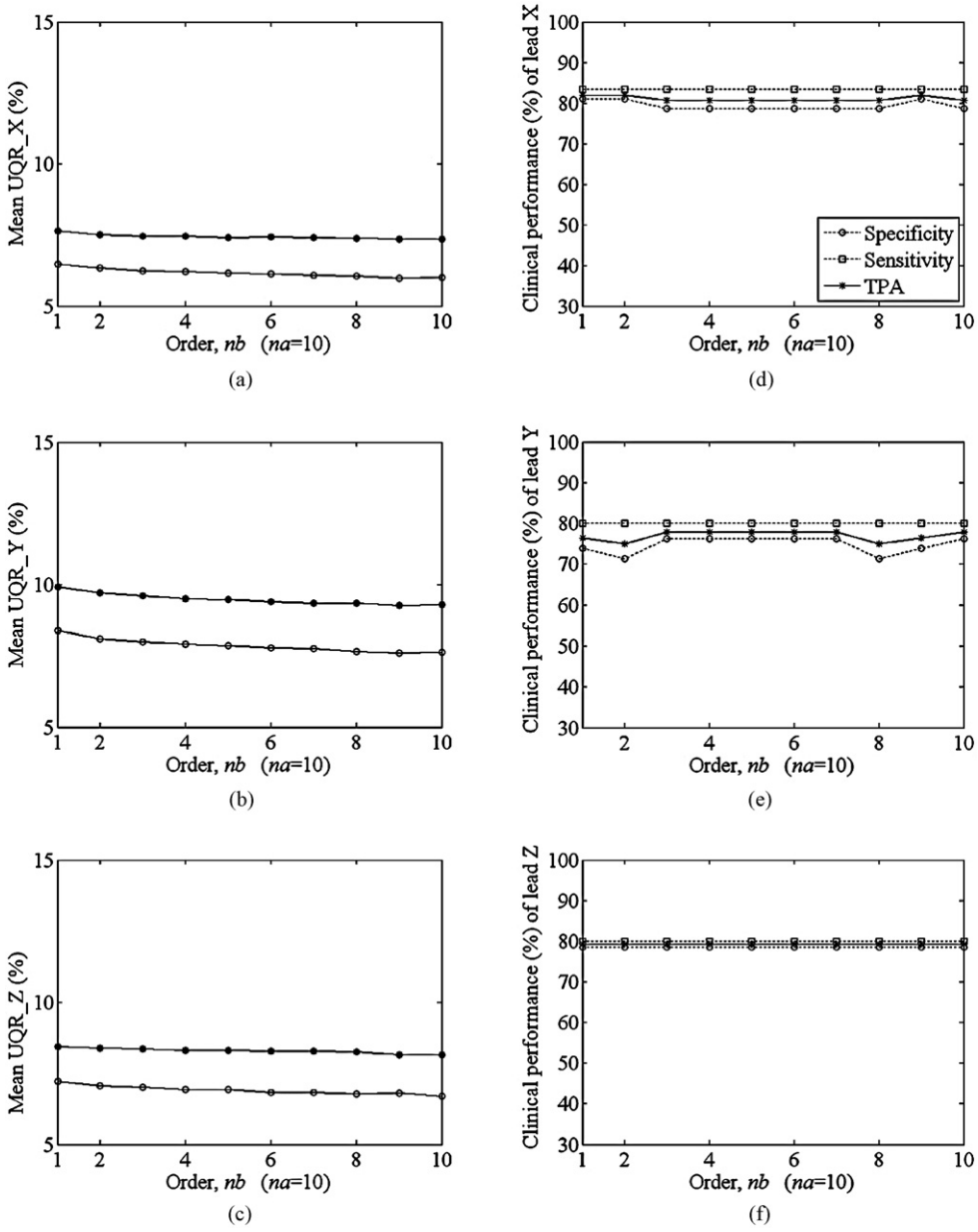

Fig. 6. Analysis of the model order *nb* vs. (a)–(c) mean UIQP-to-QRS ratios and (d)–(f) clinical performance in leads X, Y and Z. The prediction depth *k* of 6 and the order *na* of 10 are fixed.

the mean UIQP-to-QRS ratios and the clinical performance indices, including specificity, sensitivity and TPA in leads X, Y and Z for the normal and VT groups. Fig. 5(a)–(c) plots the curves of the mean UIQP-to-QRS ratios vs. the order *na* using a fixed prediction depth *k* of 6 and a fixed order *nb* of 1 in leads X, Y and Z, respectively. The increase of the order *na* can increase the prediction accuracy of the QRS complex and hence decrease the UIQP and the UIQP-to-QRS ratio. However, if the order *na* is sufficient (higher than 10), the decrease in the UIQP-to-QRS ratios is slow, and the differences between the mean UIQP-to-QRS ratios of the VT and the normal groups do not change further. Fig. 5(d)–(f) shows the curves of the clinical performance vs. the order *na* in leads X, Y and Z. If the order *na* is higher than 10, the changes in the clinical performance are small.

Fig. 6 adopts a fixed prediction depth *k* of 6 and a fixed *na* of 10, but various orders *nb* from 1 to 10. Fig. 6(a)–(c) shows that the decreases in the UIQP-to-QRS ratio are slow, and the changes in the difference between the mean UIQP-to-QRS ratios of the VT and the normal groups are small when the order *nb* is increased from 1 to 10. Fig. 6(d)–(f) shows that the changes in the clinical performance are also small. The analytical results of Figs. 5 and 6 suggest that the orders *na* = 10 and *nb* = 1 are sufficient for the analysis of UIQP.

Fig. 7(a)–(c) plots the performance curves of the prediction depth *k* vs. the clinical performance indices in leads X, Y and Z. The maximum TPA in leads X, Y and Z was 81.9%, 76.4% and 83.3% using the prediction depths of 6, 6 and 4, respectively. Too low or too high a prediction depth decreased the diagnostic performance of the VT patients.

3.3. Diagnostic performance of VT patients

Table 1 summarizes the time-domain VLP parameters, UIQP parameters and UIQP-to-QRS ratios, where the UIQPs in leads X, Y and Z were detected using an ARMA prediction model with the prediction depths of 6, 6 and 4, respectively. The results of the time-domain VLP parameters are consistent with previous stud-

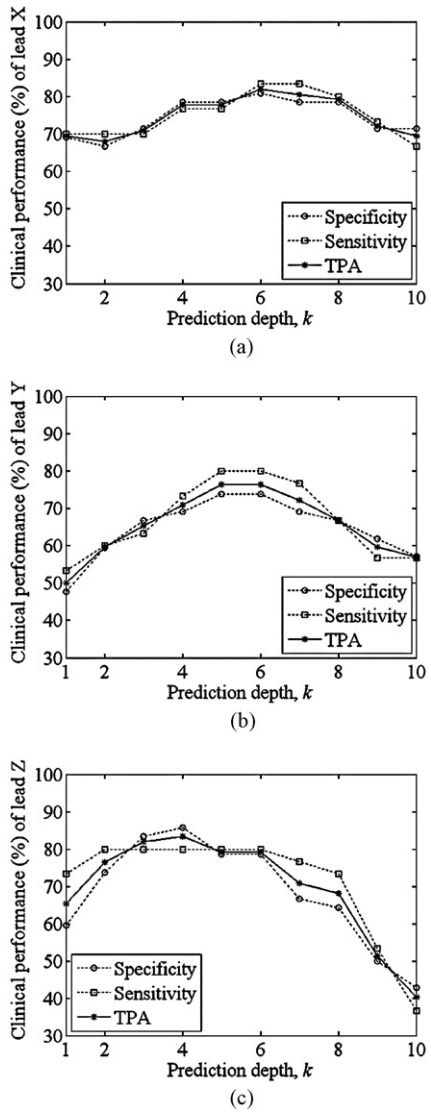

Fig. 7. Performance curves of the prediction depth k vs. the clinical performance indices in leads (a) X, (b) Y and (c) Z. The model order $na = 10$ and $nb = 1$ are fixed.

ies [15]. The RMS values of the QRS complex of VT patients were significantly lower than those of the normal group in leads Y and Z ($p < 0.05$), but not in lead X. The mean UIQP parameter of VT patients was also significantly lower than that of the normal group in lead Y ($p < 0.01$), but not in leads X and Z. All of the mean UIQP-to-QRS ratios of VT patients in leads X, Y and Z were significantly higher than those of the normal group ($p < 0.01$). The correlation analysis demonstrated significant correlations ($p < 0.01$) between QRS_X and UIQP_X ($\rho = 0.73$), QRS_Y and UIQP_Y ($\rho = 0.8$), and QRS_Z and UIQP_Z ($\rho = 0.83$) in the normal group, but no significant correlations ($p > 0.05$) between QRS_X and UIQP_X ($\rho = 0.36$), QRS_Y and UIQP_Y ($\rho = 0.37$), and QRS_Z and UIQP_Z ($\rho = -0.34$) in the VT patients. No significant correlation was shown between the UIQP parameters and gender or age ($p > 0.05$).

Table 2 lists the clinical performance indices of the time-domain VLP, the UIQP-to-QRS ratio and the synthesized parameters. The best TPAs of the individual parameters were 75.0% of RMS40 and 86.0% of UQR_Z in the time-domain VLP and UQR parameters, respectively. The linear combination of the time-domain parameters or the UQR parameters did not further increase the diagnostic performance. However the logical combination of any 4 of the UQR and time-domain parameters further increased specificity to 92.9%, sensitivity to 93.3% and TPA to 93.1%.

Table 1
Summary of time-domain, QRS, UIQP, and UQR parameters.

	Normal	VT
Time-domain parameters		
fQRSD (ms)	90.3 ± 10.2	96.5 ± 7.7**
RMS40 (μV)	43.7 ± 25.0	20.1 ± 9.6**
LAS40 (ms)	29.0 ± 5.7	37.2 ± 6.7**
QRS parameters		
QRS_X (μV)	537.7 ± 170.4	513.2 ± 299.9^{NS}
QRS_Y (μV)	625.6 ± 236.5	432.0 ± 239.8**
QRS_Z (μV)	677.8 ± 245.2	540.5 ± 253.4*
UIQP parameters		
UIQP_X (μV)	33.8 ± 9.8	33.3 ± 12.8^{NS}
UIQP_Y (μV)	51.6 ± 19.0	37.7 ± 16.7*
UIQP_Z (μV)	23.3 ± 10.0	21.1 ± 5.1^{NS}
UIQP-to-QRS ratios		
UQR_X (%)	6.5 ± 1.5	7.6 ± 2.4**
UQR_Y (%)	8.4 ± 1.4	9.9 ± 3.2**
UQR_Z (%)	3.4 ± 0.7	4.5 ± 1.5**

The UIQP of leads X, Y and Z were detected using an ARMA prediction model of order $na = 10$, $nb = 1$ with the prediction depth $k = 6$, 6 and 4, respectively. QRS_l, UIQP_l, and UQR_l are the root-mean-square value of QRS complex, unpredictable intra-QRS potentials and UIQP to QRS ratio in lead l (l is lead X, Y or Z), respectively. Student's two-tailed t-test was performed to compare the means of the two independent variables. NS, non-significant ($p > 0.05$).

* $p < 0.05$ compared to the normal group.

** $p < 0.01$ compared to the normal group.

4. Discussion

This study has demonstrated that the proposed ARMA prediction model can estimate the smoothed part of the input QRS complex, and the prediction error can be used to analyze the UIQP for the diagnosis of high-risk patients with VT. The simulation study in Fig. 2 showed that the prediction error can detect the signals with sudden slope changes as the slope changes at slope discontinuities. Although both the AIQP and the sharp QRS wave can produce sudden slope changes and cannot be further separated, the simulation results in Fig. 3 show that the presence of AIQP can increase the UIQP. Because of their abnormal myocardial conduction, the VT patients were expected to have a higher UIQP in comparison with the normal group. However the clinical results show that the mean UIQP of the VT patients was significantly lower than that of the normal group in lead Y, and no significant differences could be found in leads X and Z. This unexpected result may be caused by the amplitude variations among the study subjects, because the clinical results show the RMS values of the QRS complex in the normal and VT groups both had a wide range, from 200 μV to 1400 μV in leads X, Y and Z, and the mean RMS values of the QRS complex of the VT patients were significantly lower than those of the normal group in leads Y and Z. Moreover, because of the linearity of the ARMA prediction model, the estimated UIQPs are positively proportional to the amplitude of the input QRS complexes if the input QRS complexes have the same shapes. Hence the UIQP is not only dominated by the sharpness of the QRS wave and the AIQP, but also by the amplitude of the QRS wave.

The correlation analyses also revealed that the RMS values of the QRS complex are highly correlated with the UIQP parameters in the normal group. This may be because the sharpness of the QRS complex is similar and the AIQP is absent in the normal subjects. However, no significant correlations were found between the UIQP and the RMS value of the QRS complex in the VT patients. This may be because the estimated UIQP in the VT patients further included AIQP which was not proportional to the amplitude of the QRS wave. In view of the above, it cannot be determined that a higher UIQP

Table 2
The clinical performance indices of time-domain, UQR and synthesized parameters.

Parameters	Normal (N = 42) Specificity (%)	VT (N = 30) Sensitivity (%)	Total (N = 72) TPA (%)
Individual parameters			
fQRSD	64.3	73.3	68.1
RMS40	64.3	90.0	75.0
LAS40	71.4	70.0	70.8
UQR_X	81.0	83.3	81.9
UQR_Y	73.8	80.0	76.4
UQR_Z	85.7	80.0	83.3
Linear combination			
$-0.04 \times$ RMS40 + $0.14 \times$ LAS40	73.8	73.3	73.6
$0.19 \times$ UQR_X + $0.20 \times$ UQR_Y + $1.00 \times$ UQR_Z	90.5	73.3	83.3
$-0.02 \times$ RMS40 + $0.17 \times$ LAS40 + $0.04 \times$ UQR_X + $0.19 \times$ UQR_Y + $1.04 \times$ UQR_Z	85.7	80.0	83.3
Logical combination			
Any 2 of the UQR parameters	90.5	83.3	87.5
Any 3 of the UQR and time-domain parameters	69.0	93.3	79.2
Any 4 of the UQR and time-domain parameters	92.9	93.3	93.1
Any 5 of the UQR and time-domain parameters	97.6	66.7	84.7

TPA: total predictive accuracy; UQR_l (D) = UIQP to QRS ratio in lead l (l is lead X, Y or Z).

is induced from higher amplitude of the QRS complex or from the AIQP, even if the sharpness of the QRS complex is similar. To reduce the effect of the amplitude of the QRS complex, this study defined the UIQP-to-QRS ratio to normalize the UIQP by the RMS value of the QRS complex. An example in Fig. 4 demonstrated that a VT patient had a smaller UIQP, but showed a higher UIQP-to-QRS ratio in comparison with a normal subject. The clinical results further show that all of the mean UIQP-to-QRS ratios of the VT patients in leads X, Y and Z were significantly higher than those of the normal group. Hence the UIQP-to-QRS ratio is useful for the diagnosis of VT patients. The logical combinations of the UIQP-to-QRS ratios and the time-domain VLP parameters can further increase the diagnostic performance of VT patients.

The main difference between the UIQP analysis using the ARMA prediction model and the AIQP analysis using the ARMA model in the DCT domain is that the UIQP analysis is to detect the slope changes induced by the AIQP, while the AIQP analysis [12–15] is to extract the AIQP waveform. The study results suggest that the model order of $na = 10$ and $nb = 1$ is sufficient to analyze the UIQP (Figs. 5 and 6), and a medium prediction depth of 6 in leads X and Y, and 4 in lead Z has the best diagnostic performance for the VT patients (Fig. 7). Too small or too large a prediction depth decreases the diagnostic performance. However, no prior information can be used to determine the order of the ARMA model in the DCT domain for the AIQP analysis [12]. The estimated AIQP may also include part of the normal QRS complex because of the overlap between the AIQP and the normal QRS complex. The clinical results of the AIQP analysis are still inconsistent among several previous studies [12–15]. The study results of Gomis et al. [12] showed that the mean AIQP parameters of the VT patients (N = 59) in leads X, Y and Z were significantly higher than those of the non-VT subjects (N = 73) ($p < 0.05$). Lander et al. [13] applied the same method to 16 patients with ventricular arrhythmias and 157 subjects without ventricular arrhythmias, and the clinical results demonstrated that the mean AIQP of the arrhythmic-event group in lead X significantly exceeded that of the non-event group ($p < 0.05$); however, no significant difference of the AIQP in leads Y or Z existed between the two groups. Our previous study [14] showed that the mean AIQP of VT patients (N = 23) in lead Y was significantly lower than that of the normal subjects (N = 130) ($p < 0.05$), but that no significant differences in leads X and Z existed between the two groups. This clinical inconsistency may also be related with the effects of the amplitude variations of the QRS wave among the study subjects. Because of the linearity of the ARMA model in the DCT domain, the estimated AIQP is also proportional to the amplitude of the QRS wave if the input QRS complexes have the same shapes. Hence the AIQP analysis should also consider the effects of the amplitude of the QRS complex to reduce the clinical inconsistency.

5. Conclusions

This study has successfully demonstrated that the UIQP, defined as the signals with sudden slope changes, can be detected as the slope changes at the slope discontinuities using the ARMA prediction modeling technique. The clinical results further show that the UIQP-to-QRS ratios of VT patients were significantly higher than those of the normal group in leads X, Y and Z, and the logical combination of the UIQP-to-QRS ratios and the time-domain VLP parameters can enhance the diagnostic performance of SAECG. Hence the UIQP analysis may be a new promising method for the diagnosis of VT patients.

Conflict of interest statement

No author had a financial or personal conflict of interest related to this research or its source of funding.

Acknowledgments

The author thanks the staff of the Hemodialysis Unit and patients of the Cardiology Department at Jen-Chi General Hospital for their kind assistance and cooperation in this investigation.

Financial support: This research was supported by Taiwanese National Science Council research grant NSC97-2320-B-167-001.

References

[1] Simson MB. Use of signals in the terminal QRS complex to identify patients with ventricular tachycardia after myocardial infarction. Circulation 1981;64:235–42.
[2] Jarrett JR, Flowers NC. Signal-averaged electrocardiography: history, techniques, and clinical applications. Clin Cardiol 1991;14:984–94.
[3] Breithardt G, Cain ME, El-Sherif N, Flowers N, Hombach V, Janse M, et al. Standards for analysis of ventricular late potentials using high-resolution or signal-averaged electrocardiography: a statement by a task force committee of the European Society of Cardiology, the American Heart Association, and the American College of Cardiology. J Am Coll Cardio 1991;17:999–1006.
[4] Arnsdorf MF, Mason JW, Scheinman MM, Waldo AL. Signal-averaged electrocardiography. J Am Coll Cardiol 1996;27:238–49.
[5] Tatsumi H, Takagi M, Nakagawa E, Yamashita H, Yoshiyama M. Risk stratification in patients with Brugada syndrome: analysis of daily fluctuations in 12-lead electrocardiogram (ECG) and signal-averaged electrocardiogram (SAECG). J Cardiovasc Electrophysiol 2006;17(7):705–11.
[6] Ribeiro AL, Cavalvanti PS, Lombardi F, Nunes Mdo C, Barros MV, Rocha MO. Prognostic value of signal-averaged electrocardiogram in Chagas disease. J Cardiovasc Electrophysiol 2008;19(5):502–9.

[7] Isma'eel H, Shamseddeen W, Taher A, Gharzuddine W, Dimassi A, Alam S, et al. Ventricular late potentials among thalassemia patients. Int J Cardiol 2009;132(3):453–5.
[8] Folino AF, Bauce B, Frigo G, Nava A. Long-term follow-up of the signal-averaged ECG in arrhythmogenic right ventricular cardiomyopathy: correlation with arrhythmic events and echocardiographic findings. Europace 2006;8(6):423–9.
[9] Lander P, Berbari EJ, Rajagopalan CV, Vatterott P, Lazzara R. Critical analysis of the signal-averaged electrocardiogram Improved identification of late potentials. Circulation 1993;87(1):105–17.
[10] Schwarzmaier HJ, Karbenn U, Borggrefe M, Ostermeyer J, Breithardt G. Relation between ventricular late endocardial activity during intraoperative endocardial mapping and low amplitude signals within the terminal QRS complex on the signal-averaged surface electrocardiogram. Am J Cardiol 1990;66(3):308–14.
[11] Vaitkus PT, Kindwall KE, Marchlinski FE, Miller JM, Buxton AE, Josephson ME. Differences in electrophysiological substrate in patients with coronary artery disease and cardiac arrest or ventricular tachycardia Insights from endocardial mapping and signal-averaged electrocardiography. Circulation 1991;84(2):672–8.
[12] Gomis P, Jones DL, Caminal P, Berbari EJ, Lander P. Analysis of abnormal signals within the QRS complex of the high-resolution electrocardiogram. IEEE Trans Biomed Eng 1997;44:681–93.
[13] Lander P, Gomis P, Goyal R, Berbari EJ, Caminal P, Lazzara R, et al. Analysis of abnormal intra-QRS potentials Improved predictive value for arrhythmic events with the signal-averaged electrocardiogram. Circulation 1997;95:1386–93.
[14] Lin CC, Chen CM, Yang IF, Yang TF. Automatic optimal order selection of parametric modeling for the evaluation of abnormal intra-QRS signals in signal-averaged electrocardiograms. Med Biol Eng Comput 2005;43:218–24.
[15] Lin CC. Enhancement of accuracy and reproducibility of parametric modeling for estimating abnormal intra-QRS potentials in signal-averaged electrocardiograms. Med Eng Phys 2008;30:834–42.
[16] Berbari EJ, Bock EA, Cházaro AC, Sun X, Sörnmo L. High-resolution analysis of ambulatory electrocardiograms to detect possible mechanisms of premature ventricular beats. IEEE Trans Biomed Eng 2005;52:593–8.
[17] Lander P, Gomis P, Warren S, Hartman G, Shuping K, Lazzara R, et al. Abnormal intra-QRS potentials associated with percutaneous transluminal coronary angiography-induced transient myocardial ischemia. J Electrocardiol 2006;39:282–9.
[18] Ljung L. System identification: theory for the user, vol. 81–93. Prentice-Hall, Inc.; 1999. p. 326–329.
[19] Johnson RA, Wichern DW. Applied multivariate statistical analysis. Prentice-Hall, Inc.; 2002. p. 581–646.
[20] Griner PF, Mayewski RJ, Mushlin AI, Greenland P. Selection and interpretation of diagnostic tests and procedures. Principles and applications. Ann Intern Med 1981;94:557–92.